Special Collection

Contorted Heteroannulated Tetraareno[*a*,*d*,*j*,*m*]coronenes

Xuan Yang,[a] Frank Rominger,[a] and Michael Mastalerz*[a]

In memory of Prof. Dr. François Diederich.

Abstract: Fused polycyclic aromatic compounds are interesting materials for organic electronics applications. To fine-tune photophysical or electrochemical properties, either various substituents can be attached or heteroatoms (such as N or S) can be incorporated into the fused aromatic backbone. Coronenes and heterocoronenes are promising compounds in this respect. Up until now, the possibilities for varying the attached fused heteroaromatics at the coronene core were quite limited, and realizing both electron-withdrawing and -donating rings at the same time was very difficult. Here, a series of pyridine, anisole and thiophene annulated tetraareno[*a*,*d*,*j*,*m*]coronenes has been synthesized by a facile two-step route that is a combination of Suzuki-Miyaura cross-coupling and a following cyclization step, starting from three different diarenoperylene dibromides. The contorted molecular π-planes of the obtained *cata*-condensed tetraarenocoronenes were analyzed by single-crystal X-ray crystallography, and the photophysical and electrochemical properties were systematically investigated by UV/Vis spectroscopy and cyclovoltammetry.

Introduction

Coronene or [6]circulene, in which one benzene ring is fully surrounded by another six fused hexagonal benzenoid rings, is an often found subunit of polycyclic aromatic hydrocarbons (PAHs).[1] Since its first synthesis by Clar and co-workers in 1957,[2] fused aromatic compounds based on coronene have been intensively investigated by synthetic organic chemists and material scientists.[3] The strain-free nature makes the π-framework of coronene an ideal planar structure.[4] Further π-extensions of coronene by *peri*-condensation does not change the planarity of the central π-plane,[5] whereas multifold *cata*-condensation introduces contortion to the π-framework, because of the steric congestion caused by the generation of six cove regions at the peripheries.[6] *Cata*-condensed hexabenzocoronene (*c*-HBC) and its derivatives serve as representative examples in which the six benzene rings at the periphery displace above or below the molecular π-surface alternatingly as a result of the six cove regions.[3f,7] In comparison to their planar counterparts, contorted PAHs show increased solubilities due to reduced intermolecular aggregations, which open the possibilities to use these compounds for solution-processed applications.[8] Furthermore, due to the tendency to pack co-facially through self-complementary interactions, larger intermolecular electronic coupling and thus higher charge transport rate along the π-stacking direction in contorted coronene-based PAHs are expected. All these features make contorted PAHs good candidates for organic electronics.[7b,9]

In order to fine-tune the spectroscopic and electronic properties, heteroatoms such as nitrogen,[10] sulfur,[8f,h,i,9d,11] oxygen,[12] boron[13] or both boron and nitrogen[14] are incorporated into the backbone of coronene-based PAHs. Therefore, facile synthetic methods have been developed in recent years to obtain structurally defined heteroannulated coronenes.[3d,e,15] For instance reported Nuckolls and co-workers the synthesis of dibenzotetrathienocoronene and its derivatives in 2011,[8f] which starts with the PPh_3-mediated Ramirez reaction of 6,13-pentacenequinone with CBr_4 to give the 1,1,8,8-tetrabromobisolefin that was used in Suzuki-Miyaura cross-coupling reaction with thiophene boronic ester followed by Mallory photocyclization, to give D_{2h}-symmetric dibenzotetra-thienocoronenes in 47–90% overall yield. Another strategy to obtain *cata*-condensed tribenzotrithienocoronenes was reported by Wei and co-workers; it starts with the Suzuki-Miyaura cross-coupling reaction of 1,3,5-tri(bromomethyl)-benzene and substituted phenyl boronic acids to give 1,3,5-tribenzylbenzenes.[16] The key-step towards C_{3h}-symmetric tribenzotrithienocoronenes was a tandem Friedel-Crafts alkylation/intramolecular cyclodehydrogenation between the 1,3,5-tribenzylbenzenes and thiophene-3-carbaldehyde using $FeCl_3$ as the oxidant/Lewis acid and acetic anhydride as the dehydrating agent in a CH_2Cl_2/CH_3NO_2 mixture. Some time ago, Müllen and co-workers reported the synthesis of a three-fold quinoxalino-fused coronene based on a hexamethoxy [2.2.2]-paracyclophane.[17] The macrocycle was converted to hexa-methoxycoronene by photocyclization. Demethylation and oxidative workup gave the coronene

[a] Dr. X. Yang, Dr. F. Rominger, Prof. Dr. M. Mastalerz
Organisch-Chemisches Institut
Ruprecht-Karls-Universität Heidelberg
Im Neuenheimer Feld 270, 69120 Heidelberg (Germany)
E-mail: michael.mastalerz@oci.uni-heidelberg.de

Supporting information for this article is available on the WWW under https://doi.org/10.1002/chem.202102112

Special Collection This article belongs to a Joint Special Collection dedicated to François Diederich.

quinone, which was reacted with *o*-phenylenediamine via condensation to give the final product with D_{3h} symmetry, using a similar strategy as reported by Zinke and co-workers.[18]

Our research group has been focusing on developing new facile synthetic methods to complex aromatic π-systems by different approaches.[19] In 2016, a series of *cata*-condensed diarenoperylenes were reported based on a new synthetic route in which two additional aromatic rings are *peri*-fused to the pentacene framework by condensation of an ortho-aldehyde unit.[20] The diarenoperylenes were then regioselectively two-fold brominated, enabling the synthesis of thiophene-fused tetraareno[*a*,*d*,*j*,*m*]coronenes by palladium-catalyzed Suzuki-Miyaura cross-coupling reactions with thienyl boronic ester and subsequent photocyclization (Scheme 1).[21] In contrast to the aforementioned approaches, this one allows *cata*-condensed tetraarenocoronenes of lower symmetry (C_{2h}, without consideration of the contortion of the π-planes) to be synthesized with different fused rings (electron-withdrawing or -donating), which is presented herein.

Results and Discussion

Synthesis

According to the reactions of dibromoperylenes **1**,**2** and **7** with (5-hexylthiophen-3-yl) boronic ester as has been prior described (Scheme 1),[21] these were cross-coupled with boronic ester **10** or **15** (Scheme 2) to give the corresponding cross-coupling products in yields between 36% (**20**) and 91% (**17**). It is worth mentioning that the two methoxy groups at the pyridine ring of **15** are necessary for the successful cross-coupling reactions, as no conversion was observed when **1**, **2** or **7** were treated with 3-pyridylboronic acid instead under the same conditions, in which the transmetalation process might be suppressed by the electron-poor nature of the unsubstituted pyridyl boronic acid.[22]

The next steps are the cyclizations of the cross-coupling products **11**, **12**, **16**, **17**, **20** and **22** to the tetraarenocoronenes **13**, **14**, **18**, **19**, **21** and **23**. First, the photoreactions under the conditions similar to those used for the conversion of **3**, **4** and **8** to the thiophene-fused coronenes **5**, **6** and **9** were applied.[21] By this method, pyridine-substituted compounds **16** and **22** were photocyclized to **18** and **23** in 70 and 73% yields, respectively. However, in the series with the bismethoxy-pyridyl units, least electron-rich compound **17** is an exception, as only 26% of the fully cyclized product **19** was collected after irradiation for 16 h in the presence of 4.0 equiv. of I_2. The poor solubility of substrate **17** in cyclohexane (<0.5 μM) is responsible for the low yield, as only a small portion of the aggregated substrate particles were consumed during the reaction. Photocyclizations of 3-hexyloxyphenyl substituted compounds **11**, **12** and **20** gave even much lower yields in the photocyclization reactions and only 18% yield of **13** and 3% of **14** were isolated. Even no *cata*-condensed coronene **21** was formed after irradiating substrate **20** for 24 h in the presence of 4.0 equiv. of I_2 and excess propylene oxide.

In comparison to photocyclization reactions, intramolecular oxidative cyclodehydrogenation (Scholl reaction) is a more widely used approach to make fused PAHs by a ring-closing step.[23] Therefore, the three hexyloxyphenyl substituted compounds **11**, **12** and **20**, were subject to Scholl-type reactions using DDQ along with triflic acid (Scheme 2). The isolated yield of tetrabenzocoronene **13** was increased from 18% to 45% with part of the product lost as the phenol species.[24] It should be emphasized that the attached electron-donating 3-hexyloxy group plays a crucial role in the cyclization process, as it was found that the oxidative cyclodehydrogenation undergoes

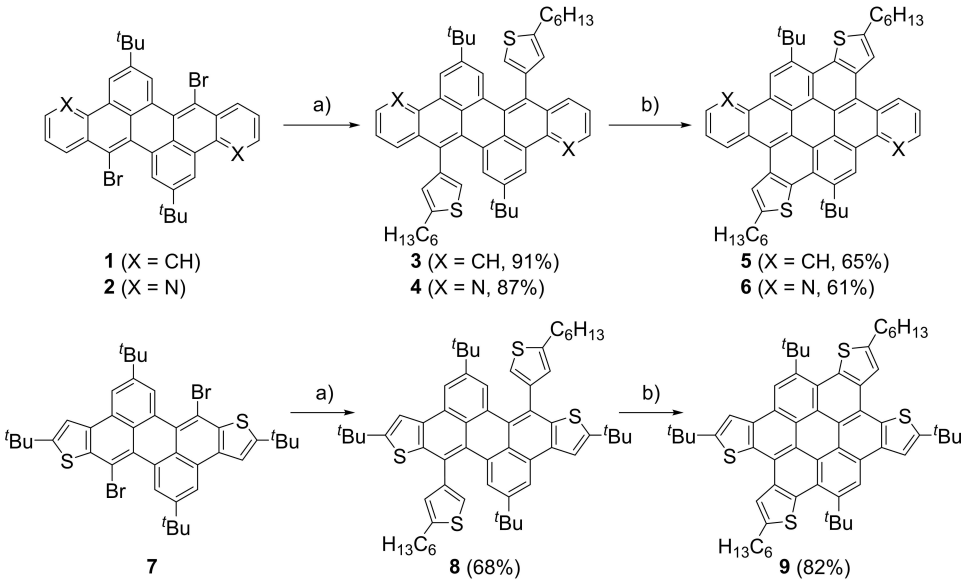

Scheme 1. Synthesis of thiophene-fused tetraarenocoronenes **5**, **6** and **9**.[21] a) (5-hexylthiophen-3-yl)boronic acid pinacol ester, 5 mol% $Pd_2(dba)_3$, 7.5 mol% tBu_3PHBF_4, 2 M K_2CO_3 (aq.), THF, 80 °C, 16 h; b) *hν*, I_2, propylene oxide, cyclohexane, 4 h. dba: dibenzylideneacetone, THF: tetrahydrofuran.

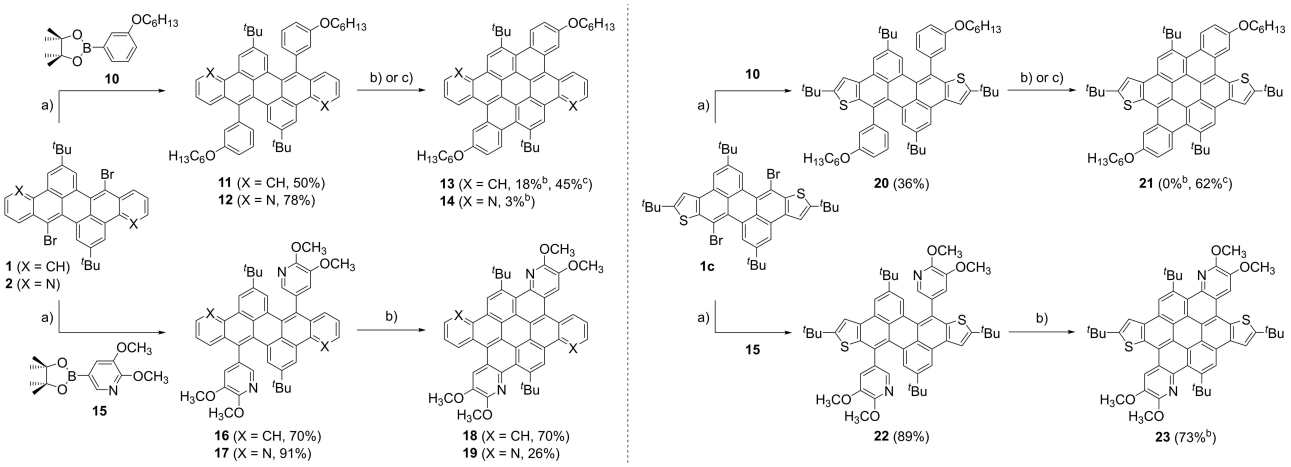

Scheme 2. Synthesis of *cata*-condensed tetraareno[*a*,*d*,*j*,*m*]coronenes **13**, **14**, **18**, **19**, **21** and **23**. a) 5 mol% $Pd_2(dba)_3$, 7.5 mol% tBu_3PHBF_4, 2 M K_2CO_3 (aq.), THF, 80 °C, 16 h; b) *hν*, I_2, propylene oxide, cyclohexane, 4–24 h; c) DDQ, TfOH, CH_2Cl_2, 0 °C, 20 min. DDQ: 2,3-dichloro-5,6-dicyano-1,4-benzoquinone, TfOH: trifluoromethanesulfonic acid.

double pentannulation if there is no substituent present on the free phenyl rings.[19e] The Scholl reaction also makes the cyclization of **20** to the dithiophene-based compound **21** possible. Treating compound **20** with 6 equiv. of DDQ in the presence of triflic acid in CH_2Cl_2 gave the doubly cyclized product **21** in 62% yield. Unfortunately, any attempts to increase the transformation of pyridine based **12** to **14** by Scholl-type conditions failed and gave only decomposition products.

Single-crystal X-ray structure analysis

High-quality single crystals of compound **13**, **14**, **21** and **23** suitable for X-ray crystallography analysis were obtained by slow vapor diffusion of CH_3OH into the sample solution in $CHCl_3$ or CH_2Cl_2.

Isosteric coronenes **13** and **14** show similar conformations and crystalline packing motifs. Both compounds crystallize in the triclinic space group *P*-1, with the molecules sitting on inversion centers. Besides the two cove regions, there is also steric repulsion between the fused hexyloxyphenyl rings and the bulky *tert*-butyl groups in both structures **13** and **14**, which make the two coronenes more contorted than the prior reported thiophene-based molecules **5**, **6** and **9**.[21] This is reflected by the dihedral angles of 27.2–28.0° of the four carbon atoms in the bay regions where the *tert*-butyl groups are attached (Figure 1a and b) being larger than those of **5**, **6** and **9** at the same positions (14.4–26.0°)[21] and that the angles between ring e at the periphery and the central ring a (28.2° for **13** and 28.4° for **14**, Figure 1d and e) are larger than those of the thiophene-fused congeners **5**, **6** and **9** (21.2–26.0°). Both structures show offset coplanar arrangements of the molecules (Figure 1g and h), which do not show any intermolecular π-stacking, but mainly pack through dispersion interactions.

Coronene **23** with both *cata*-condensed thiophene and pyridine rings, crystallizing in the monoclinic space group $P2_1/n$, shows a less twisted π-plane than **13** or **14**. The angle between the dimethoxypyridine ring e and the central ring a is 23.8° (Figure 1f). Again, no pronounced intermolecular π-stacking is observed, but molecules pack mainly via non-directional dispersion interactions. One molecule perpendicular to the crystalline lattice is surrounded by four parallel molecular dimers (Figure 1i).

Dibenzodithienocoronene **21** crystallizes in the cubic space group *Fdd*2 (Figure 2). It is interesting that the molecular contortion of **21** is different in conformation from all other coronenes described herein and published before.[21] In **21** two annulated hexyloxy-benzene rings bend towards the same side (U-shape) while the two fused thiophene rings bend towards the opposite side (S-shape) of the molecular π-plane, whereas in all other compounds it is exclusively S-shape conformations that are found. The bending deformation (the angle between the two hexyloxy chain attached benzene rings) is 56.4° (Figure 2b). Due to the negative curvature,[4b,25] **21** shows chirality and was found as a racemic crystal with two enantiomers. Two molecules sharing the same chirality (*M*,*M* or *P*,*P*) form one π-dimer (Figure 2c). In contrast to all other tetraarenocoronenes, here a distinct π-stacking distance with $d_{\pi-\pi} = 3.25$ Å is observed (Figure 2d).

By temperature-dependent ^{1}H NMR spectroscopy the interconversion energy of two enantiomers of coronene **21** was determined to be 41.5 kJ mol^{-1} (90.2 Hz) with a coalescence temperature of about −70 °C, observed with the splitting of the two signals of the $-OCH_2$ groups of the hexyloxy chains at 4.31 ppm (Figure 3).

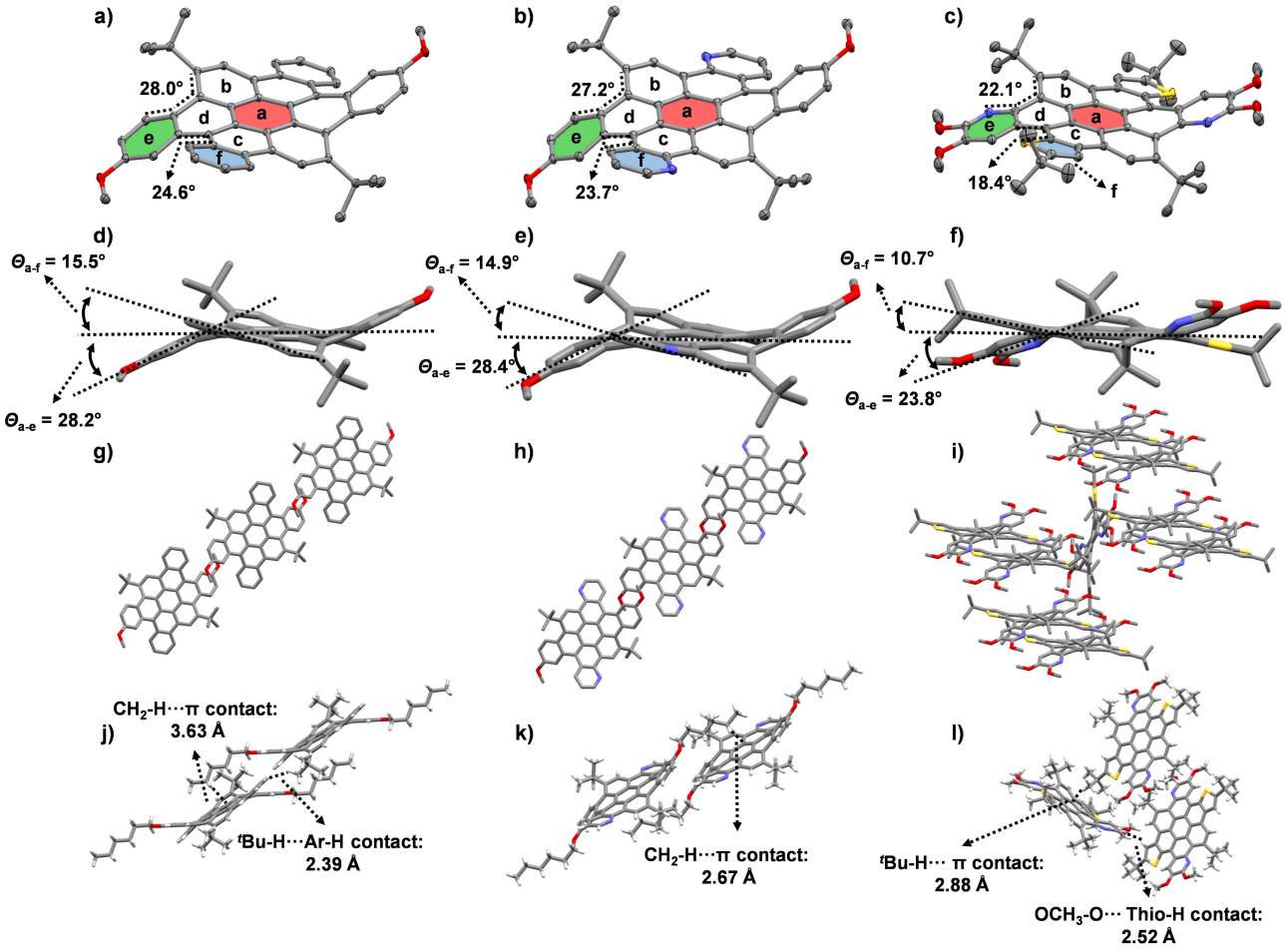

Figure 1. X-ray crystal structures of coronenes **13** (a, d, g and j), **14** (b, e, h and k) and **23** (c, f, i and l). ORTEP plots are at 50% probability. Enclathrated solvent molecules and hydrogen atoms (except in j–l) are omitted for clarity. The hexyloxy chains in a, b, d, e, g and h are replaced by methoxy groups. Colors for heteroatoms: blue = nitrogen, yellow = sulfur, red = oxygen. For detailed crystallographic data, see the Supporting Information.

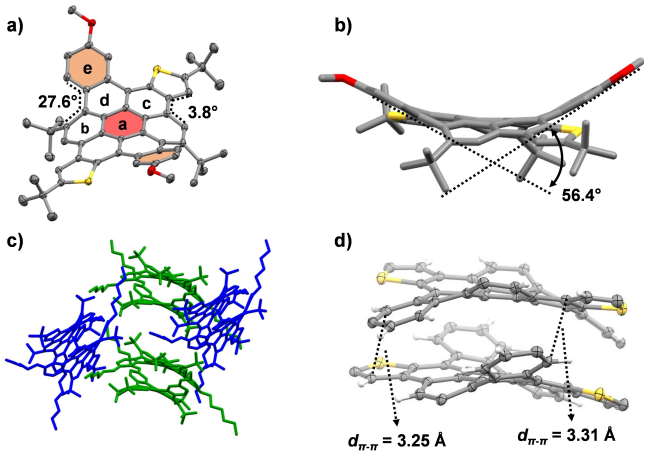

Figure 2. X-ray crystal structures of coronene **21**. ORTEP plots are at 50% probability. Enclathrated solvent molecules, hydrogen atoms (in a–c) and the *tert*-butyl groups (in d) are omitted for clarity. The hexyloxy chains are replaced by methoxy groups in a and b and omitted in d. The two enantiomers are highlighted in different colors in c. (*M*,*M*: green and *P*,*P*: blue). Colors as in Figure 1. For detailed crystallographic data, see the Supporting Information.

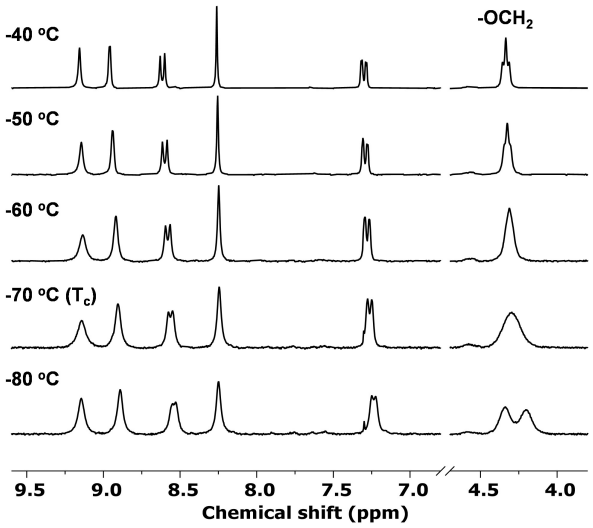

Figure 3. Variable-temperature ^{1}H NMR spectra (300 MHz, CD_2Cl_2) of coronene **21**. For full spectra, see the Supporting Information.

Spectroscopic and electrochemical properties

All precursors and the *cata*-condensed tetraarenocoronenes were investigated by photophysical and electrochemical characterizations (Figure 4 and Table 1) performed in CH_2Cl_2 at room temperature. For the sake of completeness, the data of compounds **3**–**6**, **8** and **9** will be included in this comparative discussion. Well-resolved β- and p-band (π–π* transitions) absorptions[26] are observed in the UV/Vis spectra of all compounds. For the uncyclized precursors the positions of absorption maxima depend mainly on the diarenoperylene backbones. For example, compounds **8**, **20** and **22** with the same thiophene-fused perylene backbone, show similar p-band absorption maxima at 477–478 nm. This absorption peak shows a significantly hypsochromic shift to 433 nm for the pyridine-fused compound **12**. A similar phenomenon is also found for the corresponding emission spectra. Compounds **3**, **4**, **11**, **12**, **16** and **17** emit at 472–481 nm, while the emission maxima of the thiophene-fused compounds **8**, **20** and **22** shift bathochromically to 529–533 nm.

The sharp β-band absorptions in the range of 350–370 nm with significantly increased extinction coefficients are observed in the UV/Vis absorption spectra of all tetraarenocoronenes, clearly indicating the formation of the coronene central cores by cyclodehydrogenation.[6,27] Absorption spectra predicted by the time-dependent density functional theory (TDDFT) calculations indicate that these strong β-band absorptions in the region of 345–381 nm origin from three main transitions (HOMO-1→LUMO+1, HOMO-1→LUMO and HOMO→LUMO+1) with large oscillator strengths (Figure S107–S115 and Table S5–S14). The highest extinction coefficients ($>1.60\times10^5\ M^{-1}\ cm^{-1}$) are observed for coronenes **5**, **6** and **9** with annulated hexylthiophene rings. Tetrabenzocoronene **13** without any heteroatoms in the aromatic backbone shows two β-band absorption peaks at 355 and 373 nm, along with one shoulder at 344 nm. Furthermore, two p-band absorption peaks at 422 and 447 nm were observed, with a high extinction

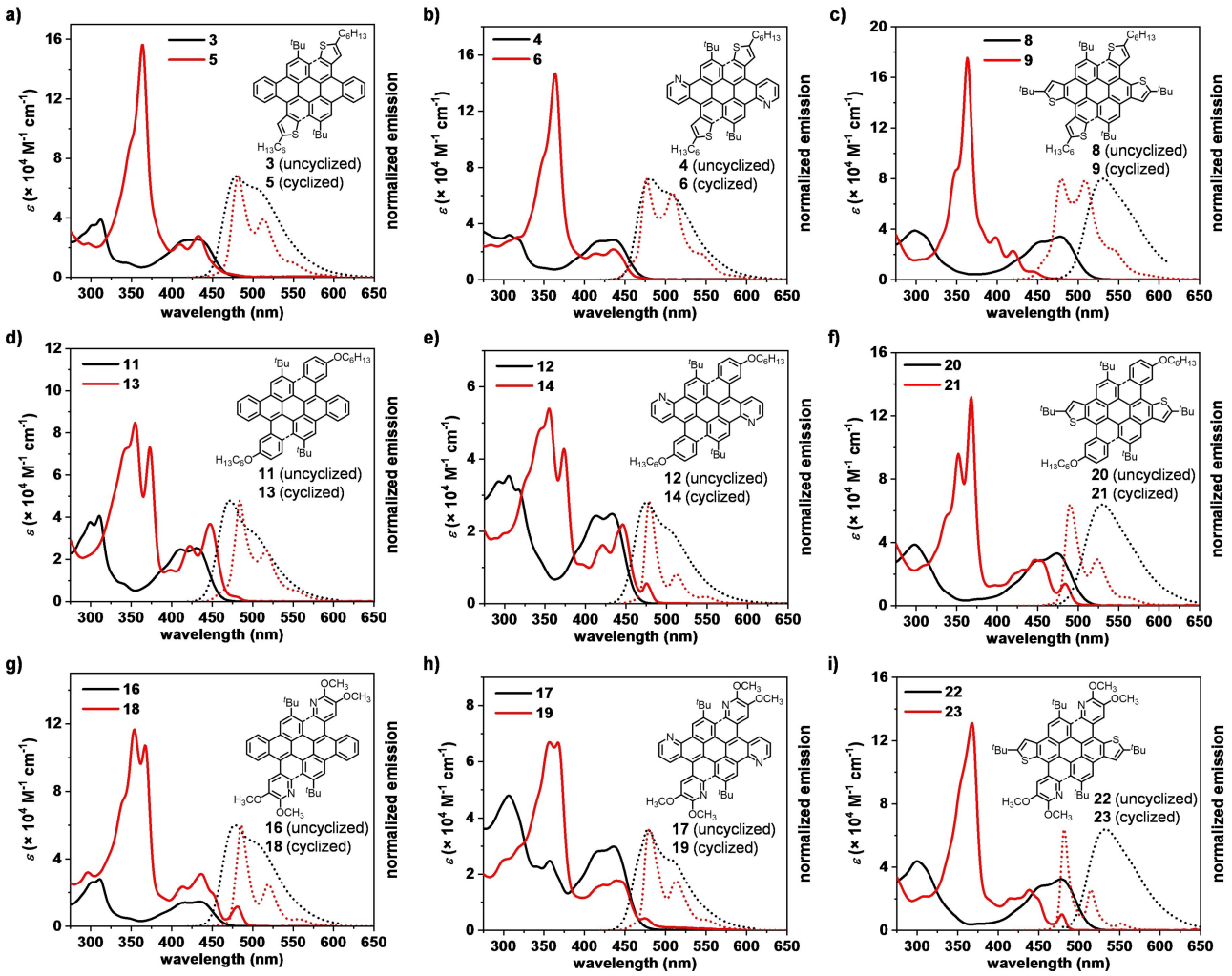

Figure 4. UV/Vis absorption (solid lines) and photoluminescence (dotted lines) spectra of the uncyclized precursors (black lines) and the corresponding tetraarenocoronenes (red lines) measured in CH_2Cl_2 (c = 4—26 μmol L^{-1}) at room temperature. The results of compounds **3**, **4** and **8** and **5**, **6** and **9** are taken from ref. [21].

Table 1. Summary of the photophysical and electrochemical characterizations of uncyclized precursors and *cata*-condensed coronenes.

Compd	λ_{abs} [nm][a,b]	λ_{em} (λ_{ex}) [nm][a]	Φ [%][a,d]	$\tilde{\nu}$ [cm^{-1}][a,c]	E_g^{opt} [eV][a,b]	IP^{CV} [eV][e,f]	EA^{CV} [eV][g]	E_g^{CV} [eV][h]	E_{HOMO}^{DFT} [eV][i]	E_{LUMO}^{DFT} [eV][i]
3[j]	302, 312, 416, 432	479, 502 (416)	14.1 ± 1	2271	2.7	−5.2	−2.5	2.7	−5.1	−2.0
4[j]	307, 317, 421, 435	481, 502 (421)	12.4 ± 0.4	2198	2.7	−5.3	−2.7	2.7	−5.2	−2.1
8[j]	298, 454, 478	531 (310)	37.7 ± 0.1	2088	2.4	−5.0	−2.6	2.4	−4.8	−1.9
11	299, 311, 341, 411, 431	472, 502 (311)	53.5 ± 1.3	2015	2.7	−5.2	−2.5	2.7	−5.1	−2.0
12	293, 305, 317, 414, 433	475, 500 (414)	55.3 ± 0.7	2042	2.7	−5.4	−2.6	2.8	−5.2	−2.1
16	302, 311, 647, 416, 435	478, 501 (311)	58.4 ± 0.6	2068	2.7	−5.3	−2.6	2.7	−5.2	−2.1
17	306, 341, 357, 418, 436	478, 506 (341)	54.4 ± 2.0	2015	2.7	−5.3	−2.6	2.7	−5.3	−2.2
20	298, 452, 474	529 (452)	76.3 ± 2.3	2193	2.4	−5.0	−2.6	2.4	−4.8	−1.9
22	300, 376, 456, 478	533 (478)	77.5 ± 1.0	2156	2.4	−5.1	−2.6	2.5	−4.9	−2.0
5[j]	296, 349, 363, 409, 433	482, 512 (363)	2.5 ± 0.1	2348	2.7	−5.2	−2.5	2.7	−5.1	−1.9
6[j]	284, 350, 364, 413, 436	476, 509 (364)	2.7 ± 0.1	1927	2.7	−5.3	−2.6	2.7	−5.3	−2.1
9[j]	350, 363, 398, 419, 442	480, 509 (363)	6.8 ± 0.1	1791	2.7	−5.1	−2.5[k]	n. d.	−5.1	−1.8
13	355, 373, 399, 422, 447	485, 517 (373)	15.0 ± 0.4	1753	2.7	−5.2	−2.6	2.6	−5.1	−2.1
14	355, 373, 421, 446, 475	479, 512 (355)	21.9 ± 0.6	1545	2.5	−5.4	−2.6	2.8	−5.2	−2.2
18	354, 367, 414, 436, 481	486, 519 (367)	35.0 ± 0.4	2360	2.5	−5.3	−3.0	2.3	−5.1	−2.0
19	357, 367, 424, 439, 475	480, 513 (367)	23.1 ± 1.2	1946	2.5	−5.4	−3.3	2.1	−5.3	−2.1
21	352, 368, 447, 454, 484	491, 524 (368)	17.5 ± 0.5	2005	2.5	−5.0	−2.6	2.4	−4.9	−1.9
23	368, 415, 438, 479	482, 515 (368)	16.4 ± 0.8	2084	2.5	−5.2	−2.5	2.6	−5.1	−2.0

[a] Measured in CH_2Cl_2 at room temperature. [b] Estimated from absorption onset. [c] Stokes's shift. [d] Fluorescence quantum yield. [e] Ionization potential. [f] Measured in 0.1 M nBu$_4$NClO$_4$ in CH_2Cl_2 at room temperature. The scan speed was 100 mV s^{-1}, and ferrocene/ferrocenium (Fc/Fc$^+$) was used as internal reference. IP^{CV} = −(E_{onset}^{ox} + 4.8 eV). EA^{CV} = −(E_{onset}^{red} + 4.8 eV). [g] Electron affinity. [h] E_g^{CV} = EA^{CV} − IP^{CV}. [i] Calculated by DFT in vacuum using Spartan 14 at the B3LYP/6-311G* level of theory. [j] Data taken from reference.[21] [k] EA^{CV} = IP^{CV} + E_g^{opt}.

coefficient of 3.68 × 10^4 M^{-1} cm^{-1} at 447 nm. Note that **13** shows the most bathochromic shift in the p-band absorption in comparison to other pyridine or thiophene annulated coronenes. In the cases of double thiophene and double pyridine fused coronenes (**6** and **23**), the β-band absorptions get sharper with only one maximum at 364 and 368 nm, respectively, while the corresponding extinction coefficients increase in comparison to the tetrabenzocoronene **13**. Tetrakispyridinocoronene **19** shows moderate intensities for both of the β- and the p-bands. For coronene **9** with four thiophene units a sharp β-band absorption peak at 363 nm with the highest extinction coefficient of 1.75 × 10^5 M^{-1} cm^{-1} in this series is detected. One characteristic absorption peak at 398 nm is observed for **9**.[8h] *Cata*-condensed coronenes with pyridine annulations (**14**, **18**, **19**, and **23**, except **6**) and negatively curved coronene **21** show α-bands (n–π* transition) at around 480 nm, of which **21** has the most bathochromically shifted maximum at 484 nm.

Emission spectra with similar patterns are found in this coronene series. One main emission peak at 476–486 nm and one second shoulder peak at 509–524 nm are observed in all cases. Coronene **21** shows the most bathochromic emission at 491 and 524 nm. In comparison to the precursors before cyclization, the fluorescence quantum yields of all coronenes decrease, while coronenes with only nitrogen doping show moderate quantum yields of over 20%.

By cyclovoltammetry the oxidation and reduction waves were measured reflecting the ionization potentials (IPs) and electron affinities (EAs) of all the precursors and the fused coronenes (Table 1 and the Supporting Information). For the tetrabenzocoronene **13**, the IP and EA are determined to be at −5.2 and −2.6 eV, respectively. The IPs of the pyridine-fused coronenes **6**, **14**, **18** and **19** are about 0.2 eV lower in energy than that of **13**, and the tetrakispyridinocoronene **19** shows the most stabilized energy levels of IP = −5.4 and EA = −3.3 eV. Annulation with thiophene rings slightly increase the IPs, in the cases of thiophene-fused molecules **5**, **9** and **21**.

DFT calculations

Structural optimizations of the nine tetraarenocoronenes in vacuum were performed based on density functional theory (DFT) calculations at the B3LYP/6-311G* level of theory.[28] The calculated levels of frontier molecular orbitals (FMOs) are summarized in Table 1 and the FMOs are depicted in Figure 5. The FMOs of tetrabenzocoronene **13** were calculated to be at E_{HOMO} = −5.09 eV and E_{LUMO} = −2.09 eV. The HOMO levels are slightly stabilized by 0.03–0.04 eV while the LUMO levels are destabilized by 0.11–0.15 eV, if the *cata*-condensed hexyloxybenzene rings are replaced by hexylthiophene (**5**) or dimethoxy-pyridine rings (**18**). Both the HOMOs and LUMOs of the pyridine-fused coronenes **6**, **14** and **19** are stabilized in comparison to the congeners of **13**, **5** and **18**, respectively, because of the electron-withdrawing nature of the pyridyl units. The substitution of benzene rings by hexylthiophene (**6**) or dimethoxypyridine rings (**19**) causes similar effects to the FMO levels compared to those of **5**, **13** and **18**, with the HOMOs getting slightly stabilized by 0.04 eV and the LUMOs destabilized by 0.07–0.09 eV. The highest HOMO level (−4.93 eV) and smallest HOMO-LUMO gap (3.01 eV) in this coronene series is found for negatively curved molecule **21**; this is consistent with the experimentally measured UV/Vis spectra and the electrochemical data. Therefore, the levels of FMOs of these nine *cata*-condensed heteroannulated coronenes mainly depend on the aromatic rings fused to the [*d*,*m*] edges of the central coronene cores. The aromatic units fused to the [*a*,*j*] edges give slightly stabilized HOMOs and destabilized LUMOs.

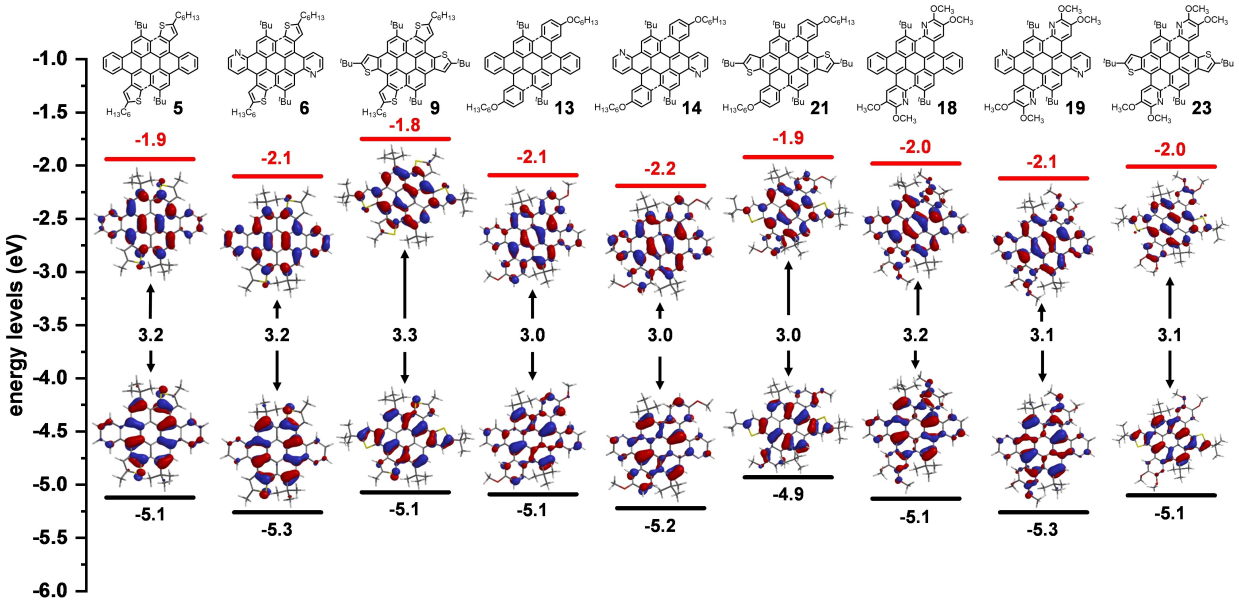

Figure 5. Calculated frontier molecular orbitals of the fused coronenes based on DFT at the B3LYP/6-311G* level of theory using Spartan 14. Black lines: HOMO, red lines: LUMO. The results of compounds **5**, **6** and **9** are taken from ref. [21]. The hexyl and hexyloxy chains were replaced by methyl or methoxy groups during the calculations for simplification.

Conclusions

Starting from three doubly brominated diarenoperylenes, *cata*-condensed heteroannulated tetraareno[*a*,*d*,*j*,*m*]coronenes with C_{2h} symmetry (assuming that the central π-planes are planar) were obtained by Suzuki-Miyaura cross-coupling and subsequent oxidative ring-closure (Mallory photocyclization or Scholl reaction). By single-crystal X-ray diffraction it was found that the tetraareno[*a*,*d*,*j*,*m*]coronenes adopt S-shaped contorted π-planes due to the formation of two cove regions and the repulsion between the bulky *tert*-butyl groups and the aromatic units at the [*a*,*j*] positions. The dibenzo[*a*,*j*]dithieno-[*d*,*m*] coronene **21** exhibits a unique negative curvature (U conformation) with two enantiomers in the solid state. The UV/Vis absorption, fluorescence emission spectra and the DFT-calculated levels of FMOs of these coronenes mainly depend on the fused aromatic units at the [*d*,*m*] edges of the coronene central core; the substituents at the [*a*,*j*] positions have less influence. The large variety of (different) fused rings in the coronene core allows the photophysical properties to be fine-tuned and thus the coronenes' possible use in organic electronics applications.

Experimental Section

Full details of synthetic procedures and characterization data, NMR spectra, mass spectra, FT-IR spectra, variable temperature ^{1}H NMR spectra of compound **21**, absorption and emission spectra, cyclovoltammograms, X-ray crystallographic data as well as the DFT computational details can be found in the Supporting Information.

Deposition Numbers 2088768 (for **23**), 2088769 (for **13**), 2088770 (for **21**), 2088771 (for **14**) contain the supplementary crystallographic data for this paper. These data are provided free of charge by the joint Cambridge Crystallographic Data Centre and Fachinformationszentrum Karlsruhe Access Structures service.

Acknowledgements

X. Y. is thankful for a PhD scholarship from the Chinese Scholarship Council (CSC). All authors are grateful for funding of this project by the Deutsche Forschungsgemeinschaft (DFG) within the collaborative research center SFB 1249 on "N-heteropolycycles as functional materials". Open Access funding enabled and organized by Projekt DEAL.

Conflict of Interest

The authors declare no conflict of interest.

Keywords: contorted PAHs · coronene · cross-coupling · photocyclization · polycyclic aromatic hydrocarbons

[1] a) R. Scholl, K. Meyer, *Ber. Dtsch. Chem. Ges. B* **1932**, *65*, 902–915; b) M. S. Newman, *J. Am. Chem. Soc.* **1940**, *62*, 1683–1687.
[2] E. Clar, M. Zander, *J. Chem. Soc.* **1957**, 4616–4619.
[3] a) J. Wu, W. Pisula, K. Müllen, *Chem. Rev.* **2007**, *107*, 718–747; b) A. Narita, X.-Y. Wang, X. Feng, K. Müllen, *Chem. Soc. Rev.* **2015**, *44*, 6616–6643; c) X. Y. Wang, X. L. Yao, K. Müllen, *Sci. China Chem.* **2019**, *62*, 1099–1144; d) X.-Y. Wang, X. Yao, A. Narita, K. Müllen, *Acc. Chem. Res.* **2019**, *52*, 2491–2505; e) M. Stępień, E. Gońka, M. Żyła, N. Sprutta, *Chem. Rev.* **2017**, *117*, 3479–3716; f) M. Ball, Y. Zhong, Y. Wu, C. Schenck, F. Ng, M. Steigerwald, S. Xiao, C. Nuckolls, *Acc. Chem. Res.* **2015**, *48*, 267–276; g) A.-F. Tran-Van, H. A. Wegner in *Polyarenes I*, Springer, Berlin, **2014**, pp. 121–157; h) J. Q. Li, Y. X. Qian, W. B. Duan, Q. D. Zeng, *Chin. Chem. Lett.* **2019**, *30*, 292–298; i) S. Kumar, Y. T. Tao, *Chem. Asian J.* **2021**, *16*, 621–647; j) J. S. Wu, *Curr. Org. Chem.* **2007**, *11*, 1220–1240.

[4] a) E. Fawcett, J. Trotter, J. M. Robertson, *Proc. R. Soc. London Ser. A* **1966**, *289*, 366–376; b) M. Rickhaus, M. Mayor, M. Juríček, *Chem. Soc. Rev.* **2017**, *46*, 1643–1660.

[5] A. Halleux, R. H. Martin, G. S. D. King, *Helv. Chim. Acta* **1958**, *41*, 1177–1183.

[6] R. Rieger, K. Müllen, *J. Phys. Org. Chem.* **2010**, *23*, 315–325.

[7] a) E. Clar, J. F. Stephen, *Tetrahedron* **1965**, *21*, 467–470; b) S. Xiao, M. Myers, Q. Miao, S. Sanaur, K. Pang, M. L. Steigerwald, C. Nuckolls, *Angew. Chem. Int. Ed.* **2005**, *44*, 7390–7394; *Angew. Chem.* **2005**, *117*, 7556–7560.

[8] a) J. P. Hill, W. Jin, A. Kosaka, T. Fukushima, H. Ichihara, T. Shimomura, K. Ito, T. Hashizume, N. Ishii, T. Aida, *Science* **2004**, *304*, 1481–1483; b) W. Jin, T. Fukushima, M. Niki, A. Kosaka, N. Ishii, T. Aida, *Proc. Natl. Acad. Sci. USA* **2005**, *102*, 10801–10806; c) Y. Yamamoto, T. Fukushima, W. Jin, A. Kosaka, T. Hara, T. Nakamura, A. Saeki, S. Seki, S. Tagawa, T. Aida, *Adv. Mater.* **2006**, *18*, 1297–1300; d) W. Jin, Y. Yamamoto, T. Fukushima, N. Ishii, J. Kim, K. Kato, M. Takata, T. Aida, *J. Am. Chem. Soc.* **2008**, *130*, 9434–9440; e) W. Zhang, W. Jin, T. Fukushima, N. Ishii, T. Aida, *Angew. Chem. Int. Ed.* **2009**, *48*, 4747–4750; *Angew. Chem.* **2009**, *121*, 4841–4844; f) C.-Y. Chiu, B. Kim, A. A. Gorodetsky, W. Sattler, S. Wei, A. Sattler, M. Steigerwald, C. Nuckolls, *Chem. Sci.* **2011**, *2*, 1480–1486; g) T. Aida, E. W. Meijer, S. I. Stupp, *Science* **2012**, *335*, 813–817; h) L. Chen, S. R. Puniredd, Y.-Z. Tan, M. Baumgarten, U. Zschieschang, V. Enkelmann, W. Pisula, X. Feng, H. Klauk, K. Müllen, *J. Am. Chem. Soc.* **2012**, *134*, 17869–17872; i) L. Chen, K. S. Mali, S. R. Puniredd, M. Baumgarten, K. Parvez, W. Pisula, S. De Feyter, K. Müllen, *J. Am. Chem. Soc.* **2013**, *135*, 13531–13537.

[9] a) X. Guo, M. Myers, S. Xiao, M. Lefenfeld, R. Steiner, G. S. Tulevski, J. Tang, J. Baumert, F. Leibfarth, J. T. Yardley, M. L. Steigerwald, P. Kim, C. Nuckolls, *Proc. Nat. Acad. Sci.* **2006**, *103*, 11452–11456; b) S. Xiao, J. Tang, T. Beetz, X. Guo, N. Tremblay, T. Siegrist, Y. Zhu, M. Steigerwald, C. Nuckolls, *J. Am. Chem. Soc.* **2006**, *128*, 10700–10701; c) X. Guo, S. Xiao, M. Myers, Q. Miao, M. L. Steigerwald, C. Nuckolls, *Proc. Nat. Acad. Sci.* **2009**, *106*, 691–696; d) A. A. Gorodetsky, C.-Y. Chiu, T. Schiros, M. Palma, M. Cox, Z. Jia, W. Sattler, I. Kymissis, M. Steigerwald, C. Nuckolls, *Angew. Chem. Int. Ed.* **2010**, *49*, 7909–7912; *Angew. Chem.* **2010**, *122*, 8081–8084; e) S. J. Kang, S. Ahn, J. B. Kim, C. Schenck, A. M. Hiszpanski, S. Oh, T. Schiros, Y.-L. Loo, C. Nuckolls, *J. Am. Chem. Soc.* **2013**, *135*, 2207–2212; f) S. Xiao, S. J. Kang, Y. Wu, S. Ahn, J. B. Kim, Y.-L. Loo, T. Siegrist, M. L. Steigerwald, H. Li, C. Nuckolls, *Chem. Sci.* **2013**, *4*, 2018–2023; g) S. Xiao, S. J. Kang, Y. Zhong, S. Zhang, A. M. Scott, A. Moscatelli, N. J. Turro, M. L. Steigerwald, H. Li, C. Nuckolls, *Angew. Chem. Int. Ed.* **2013**, *52*, 4558–4562; *Angew. Chem.* **2013**, *125*, 4656–4660; h) A. M. Hiszpanski, R. M. Baur, B. Kim, N. J. Tremblay, C. Nuckolls, A. R. Woll, Y.-L. Loo, *J. Am. Chem. Soc.* **2014**, *136*, 15749–15756; i) N. C. Davy, G. Man, R. A. Kerner, M. A. Fusella, G. E. Purdum, M. Sezen, B. P. Rand, A. Kahn, Y.-L. Loo, *Chem. Mater.* **2016**, *28*, 673–681.

[10] a) S. M. Draper, D. J. Gregg, R. Madathil, *J. Am. Chem. Soc.* **2002**, *124*, 3486–3487; b) M. Takase, V. Enkelmann, D. Sebastiani, M. Baumgarten, K. Müllen, *Angew. Chem. Int. Ed.* **2007**, *46*, 5524–5527; *Angew. Chem.* **2007**, *119*, 5620–5623; c) W. Jiang, Y. Li, W. Yue, Y. Zhen, J. Qu, Z. Wang, *Org. Lett.* **2010**, *12*, 228–231; d) E. Gońka, P. J. Chmielewski, T. Lis, M. Stępień, *J. Am. Chem. Soc.* **2014**, *136*, 16399–16410; e) A. H. Endres, M. Schaffroth, F. Paulus, H. Reiss, H. Wadepohl, F. Rominger, R. Krämer, U. H. F. Bunz, *J. Am. Chem. Soc.* **2016**, *138*, 1792–1795; f) B. Liu, D. H. Shi, Y. H. Yang, D. Y. Liu, M. Li, E. N. Liu, X. G. Wang, Q. Zhang, M. Y. Yang, J. Li, X. Y. Shi, W. L. Wang, J. F. Wei, *Eur. J. Org. Chem.* **2018**, 869–873; g) K. Oki, M. Takase, S. Mori, H. Uno, *J. Am. Chem. Soc.* **2019**, *141*, 16255–16259.

[11] a) Z. Li, L. Zhi, N. T. Lucas, Z. Wang, *Tetrahedron* **2009**, *65*, 3417–3424; b) B. He, A. B. Pun, L. M. Klivansky, A. M. McGough, Y. Ye, J. Zhu, J. Guo, S. J. Teat, Y. Liu, *Chem. Mater.* **2014**, *26*, 3920–3927; c) B. He, J. Dai, D. Zherebetskyy, T. L. Chen, B. A. Zhang, S. J. Teat, Q. Zhang, L. Wang, Y. Liu, *Chem. Sci.* **2015**, *6*, 3180–3186; d) R. Dong, M. Pfeffermann, D. Skidin, F. Wang, Y. Fu, A. Narita, M. Tommasini, F. Moresco, G. Cuniberti, R. Berger, K. Müllen, X. Feng, *J. Am. Chem. Soc.* **2017**, *139*, 2168–2171.

[12] a) E. Clar, W. Kelly, D. G. Stewart, J. W. Wright, *J. Chem. Soc.* **1956**, 2652–2656; b) M. K. Węcławski, M. Tasior, T. Hammann, P. J. Cywiński, D. T. Gryko, *Chem. Commun.* **2014**, *50*, 9105–9108.

[13] a) C. Dou, S. Saito, K. Matsuo, I. Hisaki, S. Yamaguchi, *Angew. Chem. Int. Ed.* **2012**, *51*, 12206–12210; *Angew. Chem.* **2012**, *124*, 12372–12376; b) S. Kawai, S. Saito, S. Osumi, S. Yamaguchi, A. S. Foster, P. Spijker, E. Meyer, *Nat. Commun.* **2015**, *6*, 8098; c) S. Osumi, S. Saito, C. Dou, K. Matsuo, K. Kume, H. Yoshikawa, K. Awaga, S. Yamaguchi, *Chem. Sci.* **2016**, *7*, 219–227.

[14] a) X.-Y. Wang, F.-D. Zhuang, R.-B. Wang, X.-C. Wang, X.-Y. Cao, J.-Y. Wang, J. Pei, *J. Am. Chem. Soc.* **2014**, *136*, 3764–3767; b) M. Krieg, F. Reicherter, P. Haiss, M. Ströbele, K. Eichele, M.-J. Treanor, R. Schaub, H. F. Bettinger, *Angew. Chem. Int. Ed.* **2015**, *54*, 8284–8286; *Angew. Chem.* **2015**, *127*, 8402–8404; c) G. Li, W.-W. Xiong, P.-Y. Gu, J. Cao, J. Zhu, R. Ganguly, Y. Li, A. C. Grimsdale, Q. Zhang, *Org. Lett.* **2015**, *17*, 560–563; d) X.-Y. Wang, F.-D. Zhuang, X.-C. Wang, X.-Y. Cao, J.-Y. Wang, J. Pei, *Chem. Commun.* **2015**, *51*, 4368–4371; e) K. Matsui, S. Oda, K. Yoshiura, K. Nakajima, N. Yasuda, T. Hatakeyama, *J. Am. Chem. Soc.* **2018**, *140*, 1195–1198.

[15] M. Hirai, N. Tanaka, M. Sakai, S. Yamaguchi, *Chem. Rev.* **2019**, *119*, 8291–8331.

[16] Q. Zhang, H. Peng, G. Zhang, Q. Lu, J. Chang, Y. Dong, X. Shi, J. Wei, *J. Am. Chem. Soc.* **2014**, *136*, 5057–5064.

[17] R. Rieger, M. Kastler, V. Enkelmann, K. Müllen, *Chem. Eur. J.* **2008**, *14*, 6322–6325.

[18] A. Zinke, R. Ott, M. Sobotka, R. Kretz, *Monatsh. Chem.* **1952**, *83*, 546–548.

[19] a) K. Baumgärtner, A. L. Meza Chincha, A. Dreuw, F. Rominger, M. Mastalerz, *Angew. Chem. Int. Ed.* **2016**, *55*, 15594–15598; *Angew. Chem.* **2016**, *128*, 15823–15827; b) G. Zhang, V. Lami, F. Rominger, Y. Vaynzof, M. Mastalerz, *Angew. Chem. Int. Ed.* **2016**, *55*, 3977–3981; *Angew. Chem.* **2016**, *128*, 4045–4049; c) G. Zhang, F. Rominger, M. Mastalerz, *Chem. Eur. J.* **2016**, *22*, 3084–3093; d) K. Baumgärtner, F. Rominger, M. Mastalerz, *Chem. Eur. J.* **2018**, *24*, 8751–8755; e) X. Yang, M. Hoffmann, F. Rominger, T. Kirschbaum, A. Dreuw, M. Mastalerz, *Angew. Chem. Int. Ed.* **2019**, *58*, 10650–10654; *Angew. Chem.* **2019**, *131*, 10760–10764; f) X. Yang, F. Rominger, M. Mastalerz, *Angew. Chem. Int. Ed.* **2019**, *58*, 17577–17582; *Angew. Chem.* **2019**, *131*, 17741–17746; g) T. Kirschbaum, F. Rominger, M. Mastalerz, *Angew. Chem. Int. Ed.* **2020**, *59*, 270–274; *Angew. Chem.* **2020**, *132*, 276–280; h) T. Kirschbaum, F. Rominger, M. Mastalerz, *Chem. Eur. J.* **2020**, *26*, 14560–14564; i) X. Yang, F. Rominger, M. Mastalerz, *Angew. Chem. Int. Ed.* **2021**, *60*, 7941–7946; *Angew. Chem.* **2021**, *133*, 8020–8025.

[20] G. Zhang, F. Rominger, U. Zschieschang, H. Klauk, M. Mastalerz, *Chem. Eur. J.* **2016**, *22*, 14840–14845.

[21] X. Yang, F. Rominger, M. Mastalerz, *Org. Lett.* **2018**, *20*, 7270–7273.

[22] a) M. S. Wong, X. L. Zhang, *Tetrahedron Lett.* **2001**, *42*, 4087–4089; b) H. G. Kuivila, J. F. Reuwer, J. A. Mangravite, *J. Am. Chem. Soc.* **1964**, *86*, 2666–2670; c) T. E. Barder, S. D. Walker, J. R. Martinelli, S. L. Buchwald, *J. Am. Chem. Soc.* **2005**, *127*, 4685–4696; d) N. Kudo, M. Perseghini, G. C. Fu, *Angew. Chem. Int. Ed.* **2006**, *45*, 1282–1284; *Angew. Chem.* **2006**, *118*, 1304–1306.

[23] a) M. Grzybowski, K. Skonieczny, H. Butenschön, D. T. Gryko, *Angew. Chem. Int. Ed.* **2013**, *52*, 9900–9930; *Angew. Chem.* **2013**, *125*, 10084–10115; b) M. Grzybowski, B. Sadowski, H. Butenschön, D. T. Gryko, *Angew. Chem. Int. Ed.* **2020**, *59*, 2998–3027; *Angew. Chem.* **2020**, *132*, 3020–3050; c) A. Yagi, Y. Segawa, K. Itami, *Chem* **2019**, *5*, 746–748.

[24] a) A. Zinke, R. Dengg, *Monatsh. Chem. Verw. Tl.* **1922**, *43*, 125–128; b) S. Kumar, B. Lakshmi, *Tetrahedron Lett.* **2005**, *46*, 2603–2605; c) S. Kumar, S. K. Varshney, *Synthesis* **2001**, *2001*, 0305–0311.

[25] R. B. King, *J. Phys. Chem.* **1996**, *100*, 15096–15104.

[26] a) E. Clar, *J. Chem. Phys.* **1949**, *17*, 741–742; b) E. Clar, *Spectrochim. Acta* **1950**, *4*, 116–121; c) E. Clar, *Polycyclic Hydrocarbons, Vol. 1*, Springer-Verlag, Berlin Heidelberg, **1964**.

[27] J. W. Patterson, *J. Am. Chem. Soc.* **1942**, *64*, 1485–1486.

[28] a) P. Hohenberg, W. Kohn, *Phys. Rev.* **1964**, *136*, B864-B871; b) W. Kohn, L. J. Sham, *Phys. Rev.* **1965**, *140*, A1133-A1138; c) R. G. Parr, W. Yang, *Density-Functional Theory of Atoms and Molecules*, 1st ed., Oxford University Press, New York, **1994**; d) W. Koch, *Chemist's Guide to Density Functional Theory*, 2nd ed., Wiley-VCH, Weinheim, **2001**.

Manuscript received: June 14, 2021
Accepted manuscript online: August 10, 2021
Version of record online: September 9, 2021

